Solvent Effects in the Hydrodechlorination of 2,4-Dichlorophenol over Pd/Al_2O_3

Santiago Gómez-Quero, Fernando Cárdenas-Lizana, and Mark A. Keane
Chemical Engineering, School of Engineering and Physical Sciences, Heriot-Watt University, Edinburgh EH14 4AS, Scotland

DOI 10.1002/aic.12012
Published online September 28, 2009 in Wiley InterScience (www.interscience.wiley.com).

Solvent effects in the liquid phase (0.1 MPa; 303 K) hydrodechlorination (HDC) of 2,4-dichlorophenol have been established over Pd/Al_2O_3. In the absence of secondary reactions, catalyst deactivation, and transport limitations, a stepwise HDC yields 2-chlorophenol and phenol, where product selectivity was insensitive to the nature of the solvent. In contrast, the initial HDC rates exhibited a marked dependence on the reaction medium and increased in the order: benzene < THF < n*-hexane < cyclohexane < alcohols < water. Higher rates result from the concomitant effect of an increase in the dielectric constant (ε) and a decrease in the molar volume ($\overline{v}$) of the solvent, where the major (ca. 80%) contribution is due to ε. We attribute this response to the increased solvent capacity to stabilize the arenium intermediate at higher/lower $\varepsilon/\overline{v}$, an effect that extends to reaction in water + organic combinations. We provide, for the first time, a reliable quantification of solvent effects that can be potentially applied to other catalytic hydrogenolysis systems.* © 2009 American Institute of Chemical Engineers *AIChE J,* 56: 756–767, 2010

Keywords: solvent effects in catalysis, water + alcohol mixtures, catalytic hydrodechlorination, chlorophenols, Pd/alumina

Introduction

Catalytic hydrodechlorination (HDC), the controlled removal of organic Cl with H_2, is finding increasing acceptance as a low energy, alternative chlorinated waste abatement methodology.[1] Supported palladium is now established as the most effective HDC catalyst due to its inherent capacity to promote C—Cl bond hydrogenolytic scission and resistance to deactivation by HCl.[2] Among the factors that can influence HDC performance, which include metal dispersion,[3,4] nature of the support[5] and use of additives,[6,7] solvent usage is a critical variable[8,9] that has yet to be examined in any appreciable detail. In liquid phase operations, water,[10–15] methanol,[15–19] and ethanol[19–22] have been the most commonly used solvents due to environmental applicability and/or reactant solubility considerations. The ideal role of the solvent should be, to facilitate heat transfer and/or serve as an inert reaction medium to bring the reactants in close contact.[23] Nevertheless, there is evidence in the literature demonstrating that HDC rate[10–22,24] and product distribution[15,21] can be affected by the nature of the solvent. The reason for this response is still a matter of some debate as the HDC studies that have considered the role of solvent have also exhibited (i) secondary reactions, (ii) catalyst deactivation, and (iii) mass-transfer limitations. Indeed, there are many instances where the solvent has participated in the HDC process by (a) serving as a second reactant (via H_2 donation, particularly when using iso-propanol)[25–28] or (b) reacting with the chloroaromatic leading to by-product formation.[29] In the absence of such effects, variations in HDC rate/mechanism have been linked to a solvent-dependent catalyst deactivation by the HCl by-product[16,17] where differences in solubility[30] impact on HCl removal from the catalyst surface to varying degrees.[9,21] Water/alcohol[12,13] and binary alcohol[6,18] mixtures have been used to circumvent deleterious HCl/catalyst interactions but these studies did not attempt to provide

Correspondence concerning this article should be addressed to M. A. Keane at m.a.Keane@hw.ac.uk

a quantitative relationship between the catalytic response and solvent physical/chemical properties. We should flag the work of Xia et al.[31] who studied the HDC of 2,4,4′-trichloro-2′-hydroxyphenylether over Pd/C using a range of organic solvents, linked variations in turnover frequency to solvent-reactant steric and π-resonance interactions that influenced reactant adsorption on the catalyst. The addition of a base (typically NaOH)[14,20,22] has been used to neutralize the HCl generated but lower HDC rates have also been attained and associated with active site occlusion by the precipitated chlorinated salt.[12,18] Few HDC studies have taken into consideration possible contributions due to mass-transfer limitations[19,31] with the result that the available kinetic data may be masked by H_2 and chloroaromatic transport[12,32] and/or solubility[10,15] constraints.

In this work, we have set out to address the effect of the reaction medium in the absence of secondary reactions and under negligible catalyst deactivation or transport limitations. We have considered a range of solvents (water, methanol, ethanol, *n*-propanol, THF, benzene, cyclohexane, and *n*-hexane) and solvent combinations with varying properties in terms of solvation power and solvent-solvent interactions, that is, dielectric constant, molar volume, viscosity, and enthalpy of vaporization.[23] We have chosen the HDC of 2,4-dichlorophenol (2,4-DCP) over Pd/Al_2O_3 as a suitable model catalytic reaction[33] and provide the first comprehensive quantitative treatment of HDC performance that is correlated to solvent physical/chemical characteristics.

Experimental

Materials

The 2,4-DCP reactant (Aldrich, 98.0%) and organic solvents (methanol: Riedel-de Haën, 99.9%; ethanol: Aldrich, 99.9%; *n*-propanol: Aldrich, 99.7%; THF: Aldrich, 99.9%; benzene: Aldrich, 99.9%; cyclohexane: Fluka, 99.8%; *n*-hexane: Aldrich, 99.9%) were used as received without further purification. Stock solutions with an initial 2,4-DCP concentration ($C_{2,4\text{-DCP},0}$) = 0.025 $mol_{2,4\text{-DCP}}/dm^3$ were used. The catalyst, 1.2% w/w Pd/Al_2O_3, was purchased from Sigma-Aldrich and sieved (ATM fine test sieves) into batches of 38 μm average particle diameter. A constant starting Cl/Pd molar ratio (= 900 mol_{Cl}/mol_{Pd}) was used throughout this study.

Catalyst characterization

BET surface area and pore size distribution analyses were performed using a commercial Micromeritics Flowsorb II 2300 unit. Before analysis, the samples were outgassed at 423 K for 1 h in 20 cm^3/min dry N_2. BET area was obtained in 30% v/v N_2/He (20 cm^3/min) with at least three cycles of N_2 adsorption/desorption using the standard single-point BET method. Nitrogen adsorption/desorption isotherms were performed over the relative pressure range $0.05 \leq P/P_0 \leq 0.98$, where the total pore volume and size distribution were obtained according to the method of Dollimore and Heal.[34] The BET areas and N_2 uptake/release values were reproducible to within $\pm$ 4% and the values quoted in this article are the mean. Palladium particle size and morphology were determined by transmission electron microscopy (TEM): JEOL JEM 2011 TEM unit with a UTW energy-dispersive X-ray detector (Oxford Instruments) operated at an accelerating voltage of 200 kV and using Gatan DigitalMicrograph 3.4 for data acquisition/manipulation. The samples were dispersed in acetone and deposited on a holey-carbon/Cu grid (300 Mesh). At least 650 individual Pd particles were counted and the Pd particle size quoted in this article represents the surface area-weighted mean value as explained in detail elsewhere.[35]

Catalytic procedure

The liquid phase HDC reactions were carried out in a modified, commercial glass reactor (Ken Kimble Reactors), equipped with a H_2 supply at a constant volumetric flow rate (Brooks mass flow-controlled at 150 cm^3/min) and a glass impeller providing effective agitation at 1100 rpm. We have demonstrated elsewhere[36,37] that this choice of H_2 flow and stirring speed served to minimize external H_2 transport limitations. A water-recirculating bath (Julabo HD-4) was used to stabilize the reaction temperature at $T = 303 \pm 1$ K, where loss of the reactor liquid contents in the H_2 flow was negligible (<0.5% v/v) using water as coolant (ca. 293 K). At the beginning of each experiment, the catalyst and 100 cm^3 of the stock solution were charged and agitated in a He flow (50 cm^3/min) while the temperature was allowed to stabilize (15 min), and H_2 was then introduced (time $t = 0$ for reaction). As a blank test, experiments carried out under He, that is, in the absence of H_2, did not result in any detectable conversion. A noninvasive liquid sampling via a syringe with in-line filters allowed a controlled removal of aliquots (<0.5 cm^3) from the reactor. The composition of these samples was determined by gas chromatography using a Perkin-Elmer Auto System XL GC, equipped with an FID and a DB-1 capillary column (J&W Scientific: i.d. = 0.2 mm, length = 50 m, film thickness = 0.33 μm). The concentration of organic (2,4-DCP, 2-chlorophenol (2-CP), phenol (PhOH)) and inorganic (HCl) species in the bulk liquid phase was obtained from the total molar balance in the reaction mixture, where the effect of uptake on the support was negligible.[36,38] The fractional conversion of 2,4-DCP ($X_{2,4\text{-DCP}}$) is defined as

$$X_{2,4-\text{DCP}} = \frac{C_{2,4-\text{DCP},0} - C_{2,4-\text{DCP}}}{C_{2,4-\text{DCP},0}} \tag{1}$$

where $C_{2,4\text{-DCP}}$ represents the concentration of 2,4-DCP. The selectivity to 2-CP ($S_{2\text{-CP}}$) is given with respect to the total moles of product formed.

$$S_{2-\text{CP}} = \frac{C_{2-\text{CP}}}{C_{2,4-\text{DCP},0} - C_{2,4-\text{DCP}}} \tag{2}$$

Repeated reactions with different samples of catalyst/reactant stock solution delivered raw data reproducibility that was better than $\pm$7%.

Results and Discussion

Catalyst characterization

The N_2 adsorption/desorption isotherms in Figure 1 present an hysteresis loop at high relative pressures

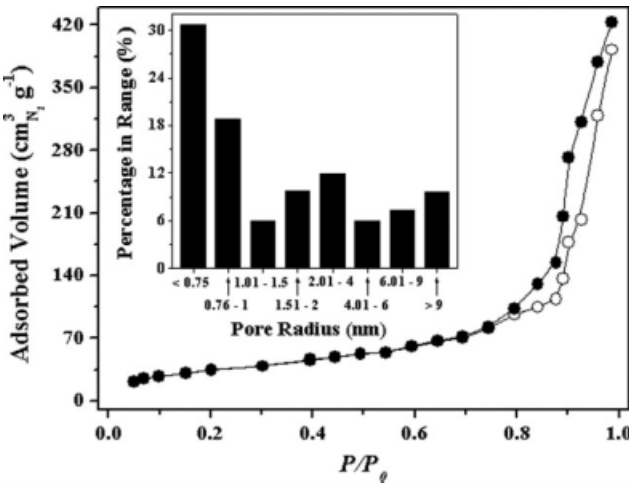

Figure 1. N_2 adsorption (○) and desorption (●) isotherms with associated pore volume distribution (inset).

($P/P_0 > 0.8$), consistent with a type IV adsorption according to the IUPAC classification, which is typical for γ-Al_2O_3.[39,40] The associated pore size distribution (see inset to Figure 1) shows significant microporous structure (pore size < 2 nm) with an appreciable contribution (35% of total volume) due to the presence of mesopores. The BET surface area (160 m^2/g) and total pore volume (0.56 cm^3/g) values are within the range reported[41] for γ-Al_2O_3-supported catalysts, that is, 150–250 m^2/g and 0.45–0.75 cm^3/g, respectively. Catalyst porosity ($\varepsilon_{catalyst}$) and tortuosity (τ) were determined according to

$$\varepsilon_{catalyst} = \rho \cdot (\text{Pore Volume}) \tag{3}$$

$$\tau = \frac{1}{\varepsilon_{catalyst}} \tag{4}$$

where ρ is the bulk density (1154 kg/m^3). The resultant values for $\varepsilon_{catalyst}$ (0.65) and τ (1.54) are indicative of low impedance with respect to reactant/product diffusion where at values approaching unity, the actual (average) path traversed by the species in the interstitial fluid within the pores is similar to that for free diffusion in the bulk fluid.[42] Representative low (a) and high (b) magnification TEM images are given in Figure 2. The Pd phase is present as well dispersed particles with a surface area-weighted mean particle size of 2.4 nm, corresponding to a specific metal surface area of 208 m^2_{Pd}/g_{Pd}.

Estimation of transport limitations

The catalytic HDC reaction requires the diffusion of both reactants to the catalyst surface and, if the rate of mass transfer is lower than that of the chemical step, a measurement of true HDC kinetics is compromised. In this three phase system, the critical mass transport steps that must be considered occur in the bulk solvent, the liquid film at the external catalyst surface and within the pores. We identify these three contributions as zones I, II, and III, respectively, and have compiled the crucial quantitative parameters that must be considered for each zone in Table 1, where we identify the critical limiting values and our actual experimental results. In zone I, transport constraints are conditioned by the solubility of both reactants in each solvent. There are no associated transport constraints for 2,4-DCP as it is soluble in each solvent (water, methanol, ethanol, *n*-propanol, THF, benzene, cyclohexane, and *n*-hexane) at the concentration (0.025 $mol_{2,4\text{-DCP}}/dm^3$) used in this study, but H_2 transport must be addressed. We have demonstrated elsewhere[36] that, at the rate of gas supply used, reaction in water is not hindered by H_2 solubility. Therefore, reaction in organic solvents will not be limited provided H_2 availability is at least equivalent to that in water. The molar fraction of H_2 (x_{H_2}) in each solvent was estimated according to the method of Prausnitz and Shair,[45] using a solubility parameter (δ) for each solvent that was calculated applying Lemcoff's relationship.[46]

$$\delta = \sqrt{\frac{\Delta\bar{H} - R \cdot T}{\bar{v}}} \tag{8}$$

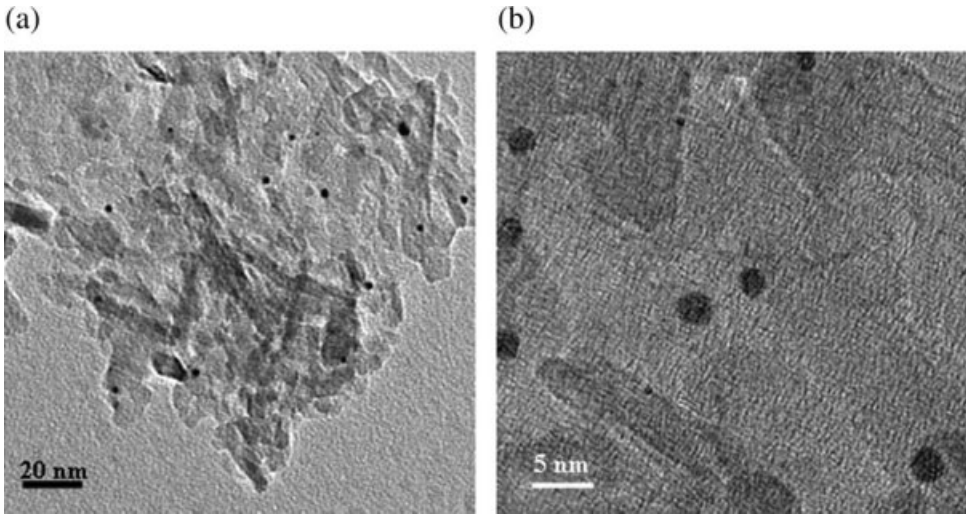

Figure 2. Representative (a) low and (b) high magnification TEM images of the Pd/Al_2O_3 catalyst.

Table 1. Summary of the Estimation of Mass Transport Resistances in the HDC of 2,4-DCP Over Pd/Al_2O_3 in Different Solvents

Zone	I (Bulk Liquid)	II (Liquid Film at the Catalyst Surface)	III (Liquid in the Catalyst Pores)
Parameter Expression	H_2 Solubility	Carberry number	Effectivenes factor
	$-\ln x_{H_2} = \ln\left(\frac{f^L_{H_2}}{f^0_{H_2}}\right) + \frac{g^2 \cdot \bar{v}_{H_2} \cdot (\delta - \delta_{H_2})^2}{R \cdot T}$ (5)	$Ca = \frac{\rho \cdot d^2}{12 \cdot m \cdot C_i \cdot D_i} \cdot (-R_i)$ (6)	$\eta = \frac{1}{\phi} \cdot \left(\frac{1}{\tanh(3\phi)} - \frac{1}{3\phi}\right)$ (7)
Variables	f^L_{H2}: fugacity of H_2 (57 MPa)*,†		ϕ: Thiele modulus
	f^0_{H2}: fugacity of H_2 (0.1 MPa)		
	g: volume fraction of the solvent ($\cong 1$)	ρ: bulk catalyst density (1154 kg/m^3)	
	$\bar{v}_{H_2}$: molar volume of H_2 (37 cm^3/mol)*,‡	d: catalyst particle diameter (38 μm)	
	δ_{H_2}: solubility parameter of H_2 (248 kJ$^{1/2}$/m$^{3/2}$)*,‡	m: catalyst concentration (0.5 g/dm^3)	
	δ: solubility parameter of the solvent (kJ$^{1/2}$/m$^{3/2}$)	C_i: bulk liquid concentration (mol/dm^3)	
	R: universal gas constant [8.314 J/(mol K)]	D_i: diffusivity (m^2/s)	
	T: temperature (303 K)	$(-R_i)$: consumption rate [mol/(g s)]	
Limiting Values	$x_{H_2} < 1 \times 10^{-5}$	$Ca > 0.1$	$\eta < 0.9$
Results	$x_{H_2} = 8 \times 10^{-5}$ to 44×10^{-5}	$Ca = 9 \times 10^{-2}$ to 5×10^{-7}	$\eta = 0.96$–1

*Value at $T = 303$ K.
†As estimated from Jáuregui-Haza et al.[43]
‡From Yen and McKetta.[44]

where $\Delta\bar{H}$ is the enthalpy of vaporization (estimated by the method of Watson),[47] and $\bar{v}$ is the molar volume (based on the Redlich-Kwong equation of state). It should be noted that the concentration of 2,4-DCP is low enough to discount any interference in the H_2 solubility calculations. The results demonstrate a wide range of H_2 molar fractions in the bulk solvent with the highest value for cyclohexane (44×10^{-5}) and lowest (8×10^{-5}) for methanol. As the range of molar fractions are well above the limiting value in water (1×10^{-5}), the available H_2 is sufficiently high that any restrictions to transport through the bulk solution are not significant. The possibility of mass transfer limitations in zone II was evaluated for both H_2 and 2,4-DCP by applying the Carberry number (Ca) approach which, assuming (i) isothermal conditions, (ii) spherical catalyst particle morphology, and (iii) the absence of concentration gradients, takes the form of the expression given in Table 1. The diffusivity of H_2 was calculated using the Wilke-Chang method[48] while 2,4-DCP diffusivity calculations were dependent on the nature of the solvent and drew on the Hayduk and Laudie equation in the case of water,[49] whereas the method of King et al.[50] was used for the organic solvents. The Ca numbers, ranging from 9×10^{-2} (2,4-DCP in water) to 5×10^{-7} (2,4-DCP in benzene), are consistent with operation under conditions of negligible reactant transport constraints. Finally, the possibility of transfer limitations in zone III was evaluated using the effectiveness factor (η, see Table 1), where the Thiele modulus (ϕ) was calculated from

$$\phi = \sqrt{\frac{(-R)_i \cdot \rho \cdot m_{Pd} \cdot (d/6)^2}{C_i \cdot D_{Eff,i}}} \quad (9)$$

where m_{Pd} represents Pd loading (0.012 g_{Pd}/g) and $D_{Eff,i}$ (m^2/s) is the effective diffusivity ($D_{Eff,i} = D_i \cdot (\varepsilon_{catalyst})^2$).[51] For each reactant/solvent system, the value of η is close to unity, indicating that the rate of transport in the catalyst pores is such that the HDC step is rate-determining. The results presented in this section confirm that the HDC of 2,4-DCP over Pd/Al_2O_3, in each of the solvents used, is free from mass transport constraints, and our catalytic data were obtained under conditions of kinetic control.

2,4-DCP HDC in single component (water or organic) solvents

The HDC of 2,4-DCP in all the solvents under consideration generated 2-CP and PhOH as the only products, resulting from partial and complete HDC, respectively. There was no evidence of 4-chlorophenol formation, hydrodeoxygenation, or ring reduction. HDC activity is expressed in terms of initial rate of 2,4-DCP consumption [$(-R_{2,4\text{-DCP}})_0$, units: $mmol_{2,4\text{-DCP}}/(g_{Pd}$ min)], as calculated from the temporal profiles for $C_{2,4\text{-DCP}}$ where $X_{2,4\text{-DCP}} = 0.25$. Under these conditions, we have demonstrated[37] that any contribution due to catalyst deactivation is negligible and the initial rate represents a true measure of the intrinsic catalyst activity. The formation of 2-CP and PhOH is possible either via a consecutive or parallel mechanism, as shown in Figure 3a. To establish the preferred HDC pathway, we applied a mass balance (in batch operation) assuming pseudo-first order kinetics for each individual step.

$$\frac{1}{W} \cdot \frac{dx_{2,4-DCP}}{dt} = -(k_1 + k_3) \cdot x_{2,4-DCP} \quad (10)$$

$$\frac{1}{W} \cdot \frac{dx_{2-CP}}{dt} = k_1 \cdot x_{2,4-DCP} - k_2 \cdot x_{2-CP} \quad (11)$$

$$\frac{1}{W} \cdot \frac{dx_{PhOH}}{dt} = k_2 \cdot x_{2-CP} + k_3 \cdot x_{2,4-DCP} \quad (12)$$

where x_i represents the molar fraction of compound i, W is the catalyst mass, and k_j is the rate constant of step j. Taking water as a representative solvent, the applicability of this model is demonstrated in Figure 3b, where the experimentally determined and predicted product compositions converge. The resultant rate constant values (in mmol/(g_{Pd} min)) are $k_1 = 385$, $k_2 = 513$, and $k_3 = 213$. The k_2/k_1 ratio (1.3) is consistent with an electrophilic aromatic substitution mechanism where

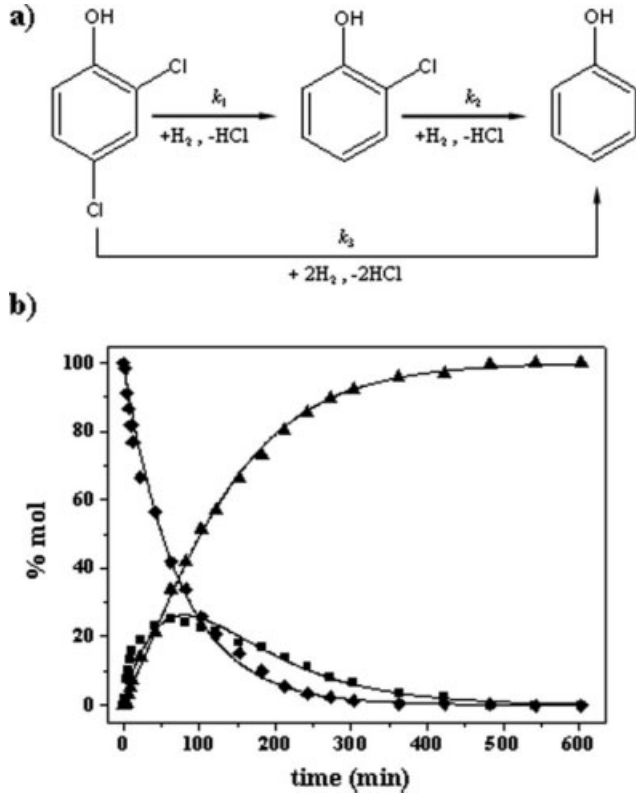

Figure 3. (a) Simplified 2,4-DCP HDC reaction scheme (stepwise pathway is highlighted in bold) and (b) bulk liquid composition as a function of reaction time, in terms of % mol 2,4-DCP (◆), 2-CP (■) and PhOH (▲) for reaction in water as solvent; lines represent fit to Eqs. 10–12.

the dechlorination rate of 2,4-DCP is lower than that of 2-CP as a result of the deactivating electron withdrawing effect of the second Cl substituent. The k_1/k_3 ratio (1.8) is indicative of a preferentially stepwise (as opposed to concerted) HDC route. The selectivity response was largely insensitive to the nature of the solvent as shown in Figure 4a where for a given fractional 2,4-DCP conversion ($X_{2,4\text{-DCP}} = 0.1$), 2-CP selectivity was essentially invariant ($S_{2\text{-CP}} = 0.77 \pm 0.04$). HDC selectivity has been reported to be both dependent[15,21] and independent[18,20] on solvent, but this response has not been discussed to any significant extent beyond reporting solvent choice to establish conditions for optimal chlorine removal. In the HDC of 4-chloroanisole over Pd/C, Ukisu and Miyadera[18] reported similar anisole selectivities (97–99%) in *i*-propanol and methanol while Cellier et al.[20] did not observe any significant selectivity dependence (96–99%) on switching from THF to ethanol. In contrast, Concibido et al.,[15] studying the HDC of tetrachloroethylene over Pd/C, proposed distinct reaction pathways in methanol and water due to the appearance of trichloroethane (as intermediate) in the former case. It is worth flagging the work of Bae et al.[21] who, taking the HDC of CCl_4 over Pd/C, recorded a selectivity to $CHCl_3$ of 97% in ethanol that was significantly higher than that (74%) obtained in acetonitrile and attributed this response to a proton-donation effect in the case of ethanol.

The initial 2,4-DCP consumption rate $[(-R_{2,4\text{-DCP}})_0]$ exhibited a strong dependence on the solvent with the following sequence of decreasing activity: water > methanol > ethanol ≈ cyclohexane ≈ *n*-hexane ≈ *n*-propanol > THF > benzene (see Figure 4b). The coupled catalytic response, that is, selectivity invariance and significant activity dependence, suggests that each HDC step (partial vs. complete HDC) is affected to the same extent in each solvent. Having established a kinetic regime, the relationship between catalytic activity and solvent properties was examined in some detail where we considered dielectric constant (ε), molar volume ($\bar{v}$), dynamic viscosity (η_S), and the boiling point enthalpy of vaporization ($\Delta\bar{H}_{T_b}$) as critical solvent properties (see Figure 5). The relevance of these properties is as follows: ε provides a measure of the capacity of the solvent to stabilize ions in solution and is linked to polarity; $\bar{v}$ represents the volume of one mole of solvent and its ability to form organized structures; η_S and $\Delta\bar{H}_{T_b}$ are the macroscopic expressions of the strength of solvent–solvent physical and chemical interactions, respectively. Our results demonstrate a dependence of $(-R_{2,4\text{-DCP}})_0$ on solvent polarity (Figure 5a) and structure (Figure 5b) but no clear relationship with respect to differences in the degree of the solvent–solvent interactions (Figures 5c,d) is apparent. HDC of 2,4-DCP proceeds via an electrophilic mechanism with the formation of a cationic reactive intermediate that is stabilized when the positive charge is delocalized due to resonance effects.[52,53] A dependence of HDC rate on the nature of the solvent can then

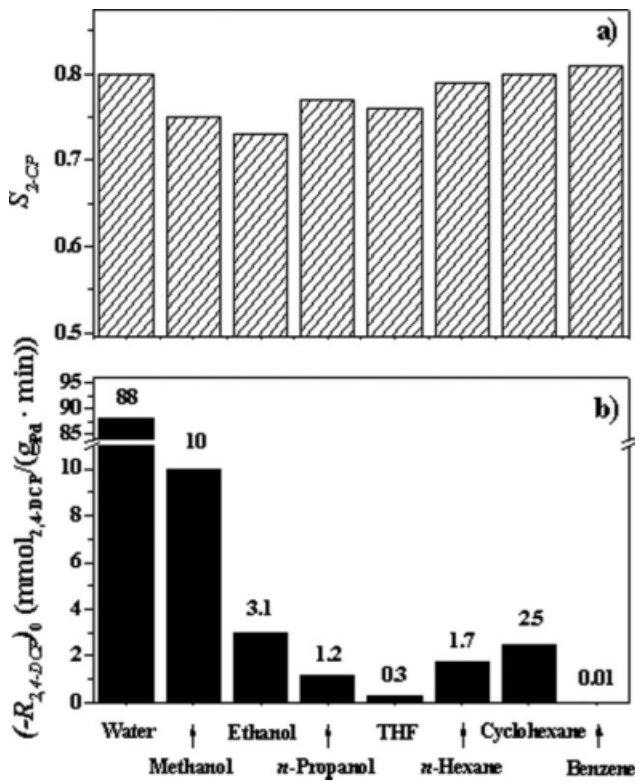

Figure 4. 2,4-DCP HDC in different solvents: (a) selectivity with respect to 2-CP ($S_{2\text{-CP}}$) at $X_{2,4\text{-DCP}} = 0.1$ and (b) initial 2,4-DCP consumption rates $[(-R_{2,4\text{-DCP}})_0]$.

result from differences in the stabilization of the electropositive intermediate due to solute–solvent interactions. The increase in $(-R_{2,4\text{-DCP}})_0$ with ε can be linked to the increased strength in the ionic (coulomb) forces due to solvation. Moreover, the increase in $(-R_{2,4\text{-DCP}})_0$ with decreasing $\bar{v}$ can be associated with the greater number of solvent molecules (per unit volume) available to interact with the charged reaction intermediate. The highest $(-R_{2,4\text{-DCP}})_0$ was observed for reaction in water, which is known to dissolve ions in solution and form well organized structures via H-bonding, that is, highest/lowest values of ε and $\bar{v}$ in Figure 5. Lower $(-R_{2,4\text{-DCP}})_0$ were recorded in those solvents (*n*-hexane, cyclohexane, benzene, and THF) with a lesser ion solvation capability and H-bonding (if any).[23]

Although there are instances in the literature where HDC rate has been linked to variations in ε,[8,17,21] this response has not been quantified. Furthermore, this is the first reported study where HDC has also been shown to vary with $\bar{v}$. As a general rule, a solvent with high ε presents a low $\bar{v}$ with the result that a decoupling of the contribution of each parameter to the observed variation in rate is not straightforward, and we could not identify any practical solvent(s) that exhibit similar ε values but differing $\bar{v}$ (or vice versa). As an alternative approach, we have adopted a mathematical solution where $(-R_{2,4\text{-DCP}})_0$ has been adjusted to the empirical relationships

$$\left(-R_{2,4-\text{DCP}}\right)_0 = a_\varepsilon \cdot (\varepsilon)^{b_\varepsilon} \tag{13}$$

$$\left(-R_{2,4-\text{DCP}}\right)_0 = a_{\bar{v}} \cdot (\bar{v})^{b_{\bar{v}}} \tag{14}$$

where a and b are fitting parameters. Given the direct and inverse dependence of $(-R_{2,4\text{-DCP}})_0$ on ε and $\bar{v}$, respectively, it follows that

$$\left(-R_{2,4-\text{DCP}}\right)_0 = a_{\text{T}} \cdot (\varepsilon/\bar{v})^{b_{\text{T}}} \tag{15}$$

and the relationship between the ε and $\bar{v}$ factors (b_{T}) can be presented as

$$b_{\text{T}} = b_\varepsilon \cdot \Psi + b_{\bar{v}} \cdot (1 - \Psi) \tag{16}$$

where Ψ serves to quantify the fractional contribution due to ε. The applicability of this approach is demonstrated in Figures 5a,b and 6, while the relevant parameters are given in Table 2. The high R^2 (0.998) illustrates the goodness of fit and the value of Ψ (ca. 0.8) establishes that the major source of the rate variation is ε. This result suggests that the strength of the solute–solvent interactions is more important than the actual (average) number of solvent molecules participating in the solvation process. In terms of practical application, in order to achieve elevated HDC rates, the choice of solvent must be prioritized, in the first instance, in terms of higher ε values where a lower $\bar{v}$ represents a secondary consideration. We believe that these findings are significant not only in terms of

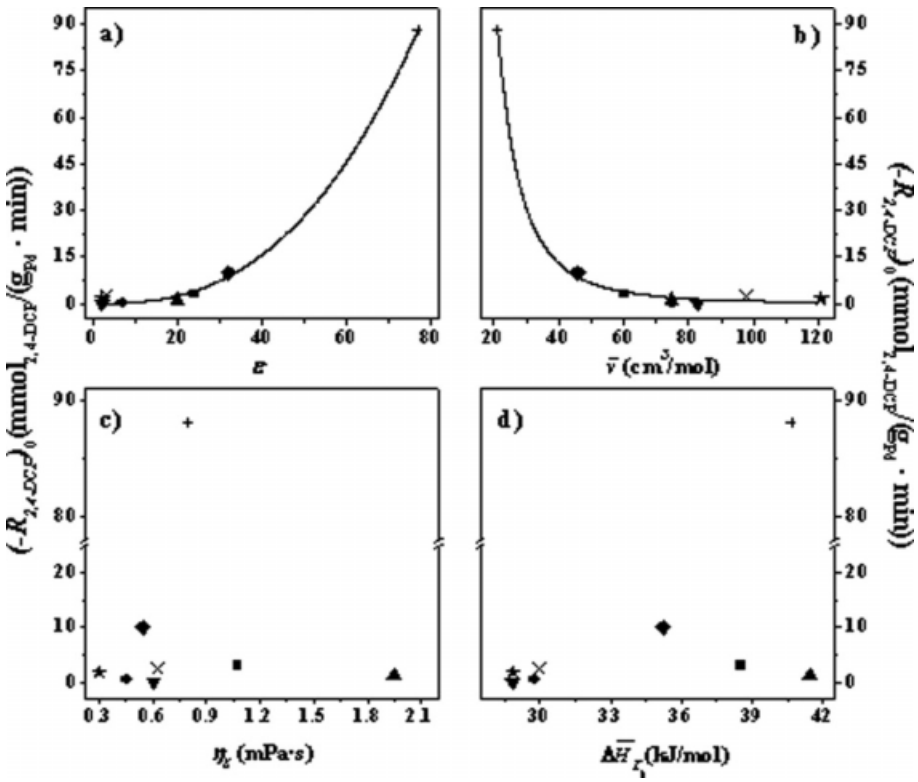

Figure 5. Initial 2,4-DCP consumption rates [$(-R_{2,4\text{-DCP}})_0$] as a function of (a) solvent dielectric constant (ε), (b) molar volume ($\bar{v}$), (c) dymanic viscosity (η_S), and (d) molar enthalpy of vaporization at normal boiling point ($\Delta\bar{H}_{T_b}$) for reaction in water (+), methanol (◆), ethanol (■), *n*-propanol (▲), THF (●), benzene (▼), cyclohexane (×), and *n*-hexane (★).

Note: lines represent fit to Eqs. 13 and 14.

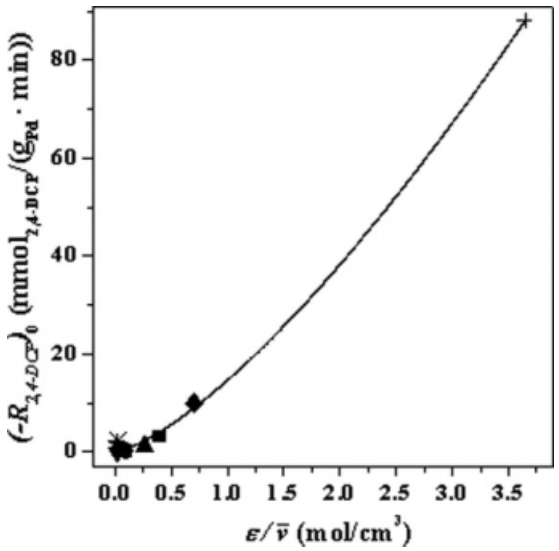

Figure 6. Initial 2,4-DCP consumption rate [$(-R_{2,4\text{-DCP}})_0$] as a function of the ratio between the solvent dielectric constant (ε) and associated molar volume ($\bar{v}$) for reaction in water (+), methanol (◆), ethanol (■), *n*-propanol (▲), THF (●), benzene (▼), cyclohexane (×), and *n*-hexane (★).

Note: line represents fit to Eq. 15.

establishing the important solvent characteristics in catalytic HDC but also as an effective quantitative approach to tackling solvent effects in catalytic systems.

2,4-DCP HDC in water + alcohol and water + THF mixtures

We have established that water is the most effective HDC solvent due to its high and low associated ε and $\bar{v}$ values, respectively. However, its applicability in a wide range of HDC reactions is limited by the low solubility of nonpolar chloroaromatics. The use of water + organic mixtures represents a compromise solution to extend the range of chloroarene concentrations that can be considered and ensure higher dechlorination rates. Such is the premise on which our study of binary solvent mixtures in 2,4-DCP HDC is based. The variation of $(-R_{2,4\text{-DCP}})_0$ in water + methanol (I), water-ethanol (II), water+*n*-propanol (III), and water+THF (IV) systems in terms of the dielectric constant of the solvent combinations (ε_m) is shown in Figure 7a. The corresponding data for single component solvents (connected by dotted lines) are identified in the figure. The impact of switching to solvent mixtures on reaction selectivity is illustrated in Figure 7b. The values of ε_m have been estimated according to

$$\varepsilon_m = (\varepsilon_{water} \cdot x_{water}) + (\varepsilon_{organic} \cdot (1 - x_{water})) \quad (17)$$

where x_{water} is the molar fraction of water in the mixture. Regardless of the organic solvent or water content, the use of aqueous + organic mixtures delivered lower $(-R_{2,4\text{-DCP}})_0$ than that predicted ($(-R_{2,4\text{-}DCP})_0^{Predicted}$) on the basis of a linear correlation of the single constituents (i.e., moving along the dotted line in Figure 7a), while all the selectivity/activity profiles were superimposable. The latter response supports our prior contention that the solvent does not influence the HDC pathway as it impacts on each individual dechlorination step to the same extent. Following our discussion in 2,4-DCP HDC in Single Component (Water or Organic) Solvents Section, the decrease in $(-R_{2,4\text{-DCP}})_0$ with dielectric constant can be linked to a lesser stabilization of the reaction intermediate. The deviation in the $(-R_{2,4\text{-DCP}})_0$ vs. ε_m profiles from the $(-R_{2,4\text{-}DCP})_0^{Predicted}$ response is significant. Indeed, there is evidence in the literature demonstrating that, when mixing water with alcohols[54–56] or THF,[57] a reorganization of the overall solution structure occurs forming co-operative domains or clusters, where water accommodates the hydrophilic/hydrophobic organic components via H-bonding/physical interactions.[54,58] The continuous formation/destruction of these domains (known as relaxation) ultimately results in an excess of the thermodynamic properties (including ε and $\bar{v}$) in the mixture. In other words, the actual values of these properties differ from those predicted on the basis of an ideal mixing rule (as assumed when using Eq. 17).[59] To assess the possible contribution of such an effect in our measurements, the excess dielectric constants (ε^E) and molar volumes ($\bar{v}^E$) were estimated by drawing on reference data.[60–63] These values were then correlated to the (negative) excess in initial 2,4-DCP consumption rate ($(-R_{2,4\text{-}DCP})_0^E$, see Figure 7aII), as defined by

$$(-R_{2,4-DCP})_0^E = (-R_{2,4-DCP})_0 - (-R_{2,4-DCP})_0^{Predicted} \quad (18)$$

The variation in ε^E and $\bar{v}^E$ with water content in the mixture is presented in Figures 8aI, aII, while the impact on $(-R_{2,4\text{-}DCP})_0^E$ is shown in Figures 8bI, bII, respectively. The occurrence of a minimum for both ε^E and $\bar{v}^E$ is well documented in the literature[58,59,64,65] for water + organic mixtures that facilitate H-bonding and is related to the formation of cooperative domains. In aqueous solutions, water molecules are arranged in tetrahedral clusters maintaining high void volumes.[59,64] If an even number of organic molecules

Table 2. Fitting Results for the Relationship Between Initial 2,4-DCP Consumption Rate $(-R_{2,4\text{-DCP}})_0$ and Dielectric Constant (b_ε), Molar Volume ($b_{\bar{v}}$), and the Ratio of Both Parameters (b_T) with Relative Uncertainties (R^2) and the Fractional Dependence on the Dielectric Constant (Ψ) for Reaction over Pd/Al_2O_3 in Different Solvents

Reaction Media	b_ε	R^2	$b_{\bar{v}}$	R^2	b_T	R^2	Ψ
Single component solvent	2.631	0.998	−3.006	0.998	1.388	0.998	0.779
Water + organic*	2.555	0.933	−3.365	0.906	1.443	0.926	0.812
Water + organic†	2.350	0.942	−2.908	0.956	1.298	0.951	0.800

*Including water + THF.
†Excluding water + THF.

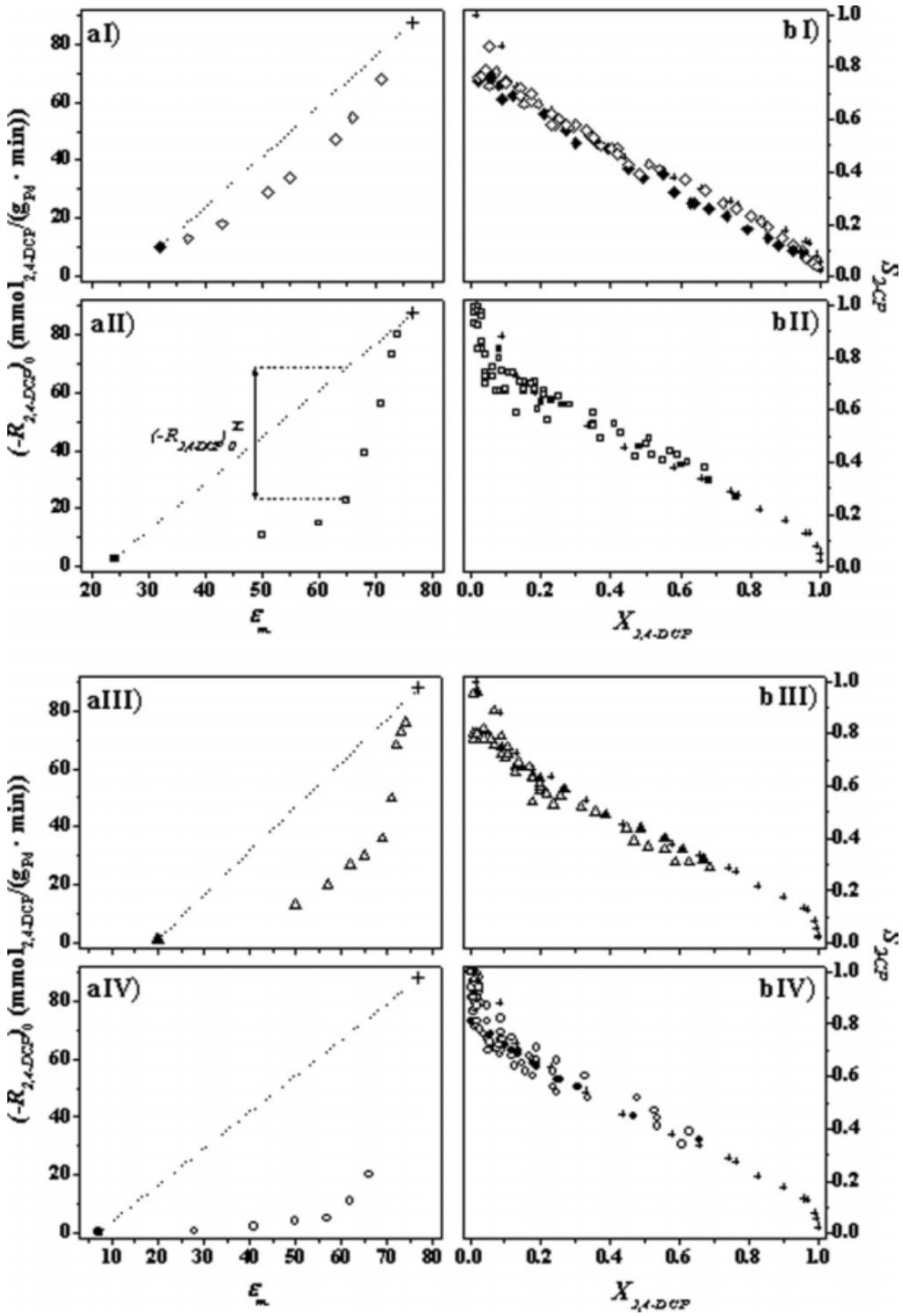

Figure 7. (a) Initial 2,4-DCP consumption rate [$(-R_{2,4\text{-DCP}})_0$] as a function of dielectric constant (ε_m) and (b) selectivity with respect to 2-CP ($S_{2\text{-CP}}$) as a function of 2,4-DCP conversion ($X_{2,4\text{-DCP}}$) for reaction in water+methanol (I, ◇), water+ethanol (II, □), water+*n*-propanol (III, Δ) and water+THF (IV, ○).

Note: dotted line connects the data for reaction in a single component solvent: water (+); methanol (◆); ethanol (■); *n*-propanol (▲); THF (●).

is introduced, water forms semiclathrate-like structures within which the organic rotates freely.[58,65] As a direct consequence, part of the void volume is lost (due to a contraction in the overall water network/structure) leading to negative values of $\overline{v}^E$ and, at the same time, the number of effective dipoles decreases resulting in a negative ε^E.[64,66] It follows that the position and extent of the minima (in terms of % mol water) are dependent on the nature of the organic component, where the lowest $\overline{v}^E$ (Figure 8aII) occurs at higher water contents when increasing the alcohol chain

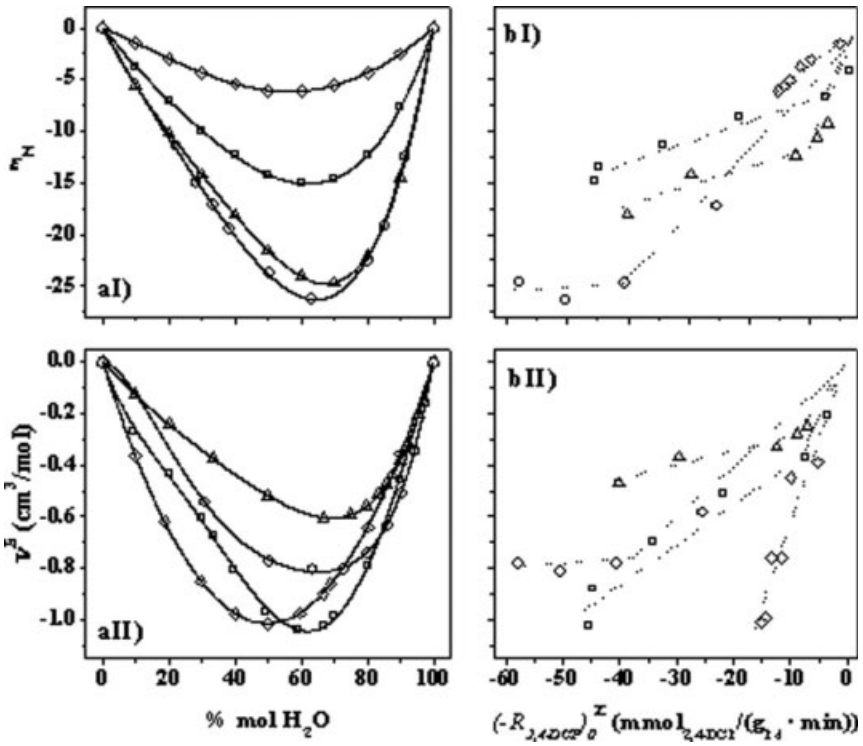

Figure 8. (a) Variation of the excess dielectric constant (ε^E, I) and excess molar volume ($\overline{v}^E$, II) of the reaction media with water content (% mol H_2O) for water + methanol (◇), water + ethanol (□), water + *n*-propanol (Δ), and water + THF (○) mixtures and (b) Relationship of the excess initial 2,4-DCP consumption rate ($(-R_{2,4\text{-}DCP})_0^E$) with ε^E (I) and $\overline{v}^E$ (II) for the same solvent mixtures.

length (methanol → *n*-propanol). Moreover, such a loss in the reaction medium structure and polarity seems to be directly related to the lower HDC activity, as can be inferred from Figure 8b, where the magnitude of $(-R_{2,4\text{-}DCP})_0^E$ is larger for mixture composition displaying larger ε^E and/or $\overline{v}^E$ values. These results suggest that, to achieve an optimum HDC rate in water + organic mixtures, the choice of water content must be made with a consideration that the composite ε and $\overline{v}$ values will be lower than those predicted from an ideal mixing rule. To assess the possible impact of the use of solvent mixtures on Ψ (the fractional contribution of ε to HDC rate), a corrected dielectric constant (ε_c) was calculated according to

$$\varepsilon_c = \varepsilon_m + \varepsilon^E \tag{19}$$

and plotted against the experimentally determined $(-R_{2,4\text{-DCP}})_0$ in Figure 9a, which also includes data for the single component solvents with fitting to Eq. 13. The same approach was also taken for an estimation of the corrected molar volume ($\overline{v}_c$, Figure 9b, fitted to Eq. 14) and $\varepsilon_c/\overline{v}_c$ (Figure 9c, fitted to Eq. 15). A visual inspection of the three graphs serves to establish the validity of our approach, where all the experimental data for single component and solvent mixtures are consistent with increasing HDC rate for decreasing $\overline{v}_c$ and increasing ε_c; the relevant fitting parameters are given in Table 2. It should be noted that water + THF mixtures deviate somewhat from the general trend, possibly a result of steric effects in the case of the bulky THF. Nevertheless, data fitting that included and excluded the water + THF dataset delivered similarly high R^2 values. This is significant, considering the possible secondary source of error associated with the ε^E and $\overline{v}^E$ values taken from the literature. The extracted (applying Eq. 16) value of Ψ (0.81) for all the solvent mixtures considered is very close to that obtained for HDC in single component solvent media. This result establishes that the critical solution property controlling HDC rate is the extent of solvent–solute interaction.

This study represents a novel systematic approach to examine solvent effects associated with liquid phase catalytic HDC, where higher rates were consistently obtained with reaction media characterized by higher ε and $\overline{v}$ plays a secondary role. This analysis is valid for both single component and binary solvent mixtures. These findings warrant further study to establish the generic features of this approach when dealing with solvent effects in liquid phase heterogeneous catalysis.

Conclusions

We have provided, for the first time, a comprehensive quantitative analysis of solvent effects in the liquid phase (at 0.1 MPa and 303 K) HDC of 2,4-DCP over Pd/Al_2O_3 using water, methanol, ethanol, *n*-propanol, THF, benzene, cyclohexane, and *n*-hexane as reaction media. We have established conditions, where catalytic HDC was conducted under chemical/kinetic control, free from mass transport, and diffusion constraints. In the absence of secondary reactions and

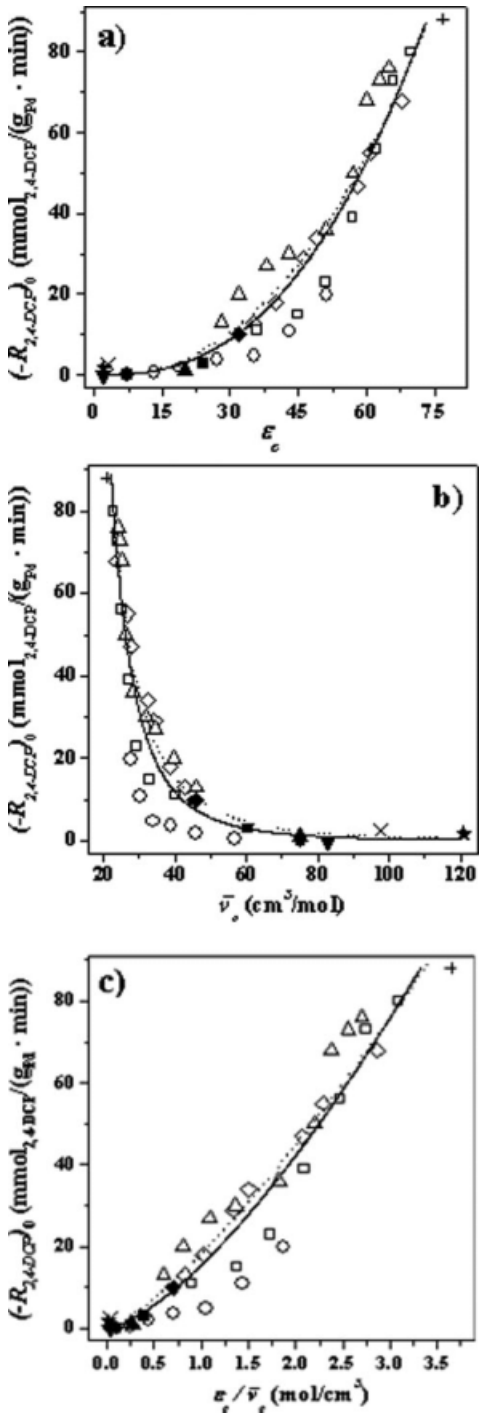

Figure 9. Initial 2,4-DCP consumption rate [$(-R_{2,4\text{-DCP}})_0$] as a function of (a) the corrected dielectric constant of the solvent (ε_c), (b) the corrected molar volume of the solvent ($\bar{v}_c$), and (c) the ratio of both properties ($\varepsilon_c/\bar{v}_c$) for single component [water (+), methanol (◆), ethanol (■), *n*-propanol (▲), THF (●), benzene (▼), cyclohexane (×), and *n*-hexane (★)] and binary water + organic mixtures [water + methanol (◇), water + ethanol (□), water + *n*-propanol (Δ), and water + THF (○)].

Note: lines represent fits for all solvents including (dotted line) and excluding (solid line) water + THF mixtures according to Eqs. 13–15.

negligible catalyst deactivation, 2-CP and PhOH were generated as products of partial and complete HDC via an electrophilic mechanism. Although reaction selectivity was insensitive to the nature of the solvent, the initial 2,4-DCP consumption rate increased in the order: benzene < THF < *n*-hexane < cyclohexane < alcohols < water. Higher HDC rates were obtained in solvents with higher dielectric constants (ε in the range 2–77) and/or lower molar volumes ($\bar{v}$ in the range 20–120 cm^3/mol). Our analysis of HDC kinetics has revealed that the major (ca. 80%) contribution to the observed HDC rate variation is ε. We attribute this response to stronger ionic forces (at higher ε) that serve to stabilize the electropositive arenium intermediate. This contribution is more important than the actual number of molecules available for solvation. This effect extends to reaction in water + alcohol and water + THF mixtures. The results establish (quantitatively) solvent effects associated with the catalytic hydrotreatment of 2,4-DCP, and our treatment represents a new approach in studying the role of solvent in liquid phase hydrogenolysis reactions.

Acknowledgments

The authors thank E. Díaz and Z.M. de Pedro for assistance in the estimation of mass transfer constraints and acknowledge financial support from EPSRC through grant No. 0231 110525.

Notation

a_ε = fitting parameter, [mmol$_{2,4\text{-DCP}}$/(g$_{Pd}$ min)]
$a_{\bar{v}}$ = fitting parameter, [(mmol$_{2,4\text{-DCP}}$ mol$_{Solvent}^{b_{\bar{v}}}$)/(g$_{Pd}$ min cm$^{3+b_{\bar{v}}}$)]
a_T = fitting parameter, [(mmol$_{2,4\text{-DCP}}$ cm$^{3+b_T}$)/(g$_{Pd}$ min mol$_{Solvent}^{b_T}$)]
b_ε = HDC rate dependence on solvent dielectric constant
$b_{\bar{v}}$ = HDC rate dependence on solvent molar volume
b_T = HDC rate dependence on both solvent dielectric constant and molar volume
Ca = Carberry number
$C_{2\text{-CP}}$ = concentration of 2-CP (mol$_{2\text{-CP}}$/dm^3)
$C_{2,4\text{-DCP}}$ = concentration of 2,4-DCP (mol$_{2,4\text{-DCP}}$/dm^3)
$C_{2,4\text{-DCP},0}$ = initial concentration of 2,4-DCP (mol$_{2,4\text{-DCP}}$/dm^3)
D_i = diffusivity of compound i (m^2/s)
$D_{Eff,i}$ = effective diffusivity of compound i (m^2/s)
d = catalyst particle diameter (m)
$\Delta\bar{H}$ = enthalpy of vaporization (kJ/mol)
$\Delta\bar{H}_{T_b}$ = boiling point enthalpy of vaporization (kJ/mol)
$f_{H_2}^{\emptyset}$ = fugacity of H_2 (MPa)
f_{H2}^{L} = fugacity of H_2 (MPa)
g = volume fraction of the solvent
k_j = pseudo-first order rate constant of step j, [mmol/(g$_{Pd}$ min)]
m = catalyst concentration (g/dm^3)
m_{Pd} = catalyst Pd loading (g$_{Pd}$/g)
P/P_0 = relative pressure
R = universal gas constant [J/(mol K)]
$(-R_i)$ = consumption rate [mol/(g s)]
$(-R_{2,4\text{-DCP}})_0$ = initial 2,4-DCP consumption rate [mmol$_{2,4\text{-DCP}}$/(g$_{Pd}$ min)]
$(-R_{2,4\text{-}DCP})_0^E$ = excess initial 2,4-DCP consumption rate in a water + organic solvent mixture, [mmol$_{2,4\text{-DCP}}$/(g$_{Pd}$ min)].
$(-R_{2,4\text{-}DCP})_0^{Predicted}$ = initial 2,4-DCP consumption rate in a water + organic solvent mixture, as predicted assuming an ideal mixing rule [mmol$_{2,4\text{-DCP}}$/(g$_{Pd}$ min)]
$S_{2\text{-CP}}$ = selectivity with respect to 2-CP
T = temperature (K)
t = time (min)

W = catalyst mass (g)
x_i = molar fraction of compound i
$X_{2,4\text{-DCP}}$ = conversion of 2,4-DCP

Greek letters

δ = solubility parameter for the solvent ($kJ^{1/2}/m^{3/2}$)
δ_{H_2} = solubility parameter for H_2 ($kJ^{1/2}/m^{3/2}$)
ε = dielectric constant
ε_c = corrected dielectric constant of a water + organic solvent mixture
$\varepsilon_{catalyst}$ = catalyst porosity
ε_m = dielectric constant of a water + organic solvent mixture
$\varepsilon_{organic}$ = dielectric constant of an organic solvent
ε_{water} = dielectric constant of water
ε^E = excess dielectric constant of a water + organic solvent mixture
η = effectiveness factor
η_S = dynamic viscosity (mPa s)
$\overline{v}$ = molar volume of the solvent (cm^3/mol)
$\overline{v}_c$ = corrected molar volume of a water + organic solvent mixture (cm^3/mol)
$\overline{v}_{H_2}$ = molar volume of H_2 (cm^3/mol)
$\overline{v}^E$ = excess molar volume of a water + organic solvent mixture (cm^3/mol)
ρ = catalyst bulk density (kg/m^3)
τ = catalyst tortuosity
ϕ = Thiele modulus
Ψ = HDC fractional dependence on dielectric constant

Literature Cited

1. Pirkanniemi K, Sillanpää M. Heterogeneous water phase catalysis as an environmental application: a review. *Chemosphere*. 2002;48: 1047–1060.
2. Urbano FJ, Marinas JM. Hydrogenolysis of organohalogen compounds over palladium supported catalysts. *J Mol Catal Chem.* 2001;173:329–345.
3. Gómez-Sainero LM, Seoane XL, Fierro JLG, Arcoya A. Liquid-phase hydrodechlorination of CCl_4 to $CHCl_3$ on Pd/carbon catalysts: nature and role of Pd active species. *J Catal*. 2002;209:279–288.
4. Aramendia MA, Boráu V, García IM, Jiménez C, Lafont F, Marinas A, Marinas JM, Urbano FJ. Influence of the reaction conditions and catalytic properties on the liquid-phase hydrodechlorination of chlorobenzene over palladium-supported catalysts: activity and deactivation. *J Catal*. 1999;187:392–399.
5. Toebes ML, van Dillen JA, de Jong KP. Synthesis of supported palladium catalysts. *J Mol Catal Chem*. 2001;173:75–98.
6. Mitoma Y, Tasaka N, Takase M, Masuda T, Tashiro H, Egashira N, Oki T. Calcium-promoted catalytic degradation of PCDDs, PCDFs, and coplanar PCBs under a mild wet process. *Environ Sci Technol.* 2006;40:1849–1854.
7. Evdokimova G, Zinovyev S, Perosa A, Tundo P. Selectivity issues in the catalytic multiphase reduction of functionalized halogenated aromatics over Pd/C, Pt/C and raney-Ni. *Appl Catal A*. 2004; 271:129–136.
8. Lassová L, Lee HK, Hor TSA. Catalytic hydrodechlorination of chlorobenzenes: effect of solvent on efficiency and selectivity. *J Mol Catal Chem*. 1999;144:397–403.
9. Concibido NC, Okuda T, Nishijima W, Okada M. Making the liquid-phase catalytic hydrodechlorination of PCE over Pd/C safer. *React Kinet Catal Lett*. 2006;89:369–376.
10. Monguchi Y, Kume A, Hattori K, Maegawa T, Sajiki H. Pd/C-Et_3N-mediated catalytic hydrodechlorination of aromatic chlorides under mild conditions. *Tetrahedron*. 2006;62:7926–7933.
11. Benítez JL, del Angel G. Catalytic hydrodechlorination of chlorobenzene in the liquid phase. *React Kinet Catal Lett*. 1999;66:13–18.
12. Xia C, Xu J, Wu W, Liang X. Pd/C-catalyzed hydrodehalogenation of aromatic halides in aqueous solutions at room temperature under normal pressure. *Catal Commun*. 2004;5:383–386.
13. Wee HY, Cunningham JA. Palladium-catalyzed hydrodehalogenation of 1,2,4,5-tetrachlorobenzene in water-ethanol mixtures. *J Hazard Mater*. 2008;155:1–9.
14. Hara T, Kaneta T, Mori K, Mitsudome T, Mizugaki T, Ebitani K, Kaneda K. Magnetically recoverable heterogeneous catalyst: palladium nanocluster supported on hydroxyapatite-encapsulated γ-Fe_2O_3 nanocrystallites for highly efficient dehalogenation with molecular hydrogen. *Green Chem*. 2008;9:1246–1251.
15. Concibido NC, Okuda T, Nakano Y, Nishijima W, Okada M. Enhancement of the catalytic hydrodechlorination of tetrachloroethylene in methanol at mild conditions by water addition. *Tetrahedron Lett*. 2005;46:3613–3617.
16. Concibido NC, Okuda T, Nishijima W, Okada M. Kinetics of deactivation of Pd/C catalyst repeteadly used in the liquid-phase hydrodechlorination of PCE. *React Kinet Catal Lett*. 2007;90:127–136.
17. Concibido NC, Okuda T, Nishijima W, Okada M. Deactivation and reactivation of Pd/C catalysts used in repeated batch hydrodechlorination of PCE. *Appl Catal B*. 2007;71:64–69.
18. Ukisu Y, Miyadera T. Catalytic dechlorination of aromatic chlorides with Pd/C catalyst in alkaline 2-propanol: activity enhancement by the addition of methanol. *React Kinet Catal Lett*. 2006;89:341–347.
19. Nishijima W, Ochi Y, Tsai TY, Nakano Y, Okada M. Catalytic hydrodechlorination of chlorinated ethylenes in organic solvents at room temperature and atmospheric pressure. *Appl Catal B*. 2004; 51:135–140.
20. Cellier PP, Spindler JF, Taillefer M, Cristau HJ. Pd/C-catalyzed room-temperature hydrodehalogenation of aryl halides with hydrazine hydrochloride. *Tetrahedron Lett*. 2003;44:7191–7195.
21. Bae JW, Jang EJ, Jo DH, Lee JS, Lee KH. Liquid-phase hydrodechlorination of CCl_4 in a medium of ethanol with co-production of acetal and diethyl acetate. *J Mol Catal Chem*. 2003;206:225–238.
22. Ukisu Y, Miyadera T. Hydrogen-transfer hydrodehalogenation of aromatic halides with alcohols in the presence of noble metal catalysts. *J Mol Catal Chem*. 1997;125:135–142.
23. Stoye D. *Ullmann's Encyclopedia of Industrial Chemistry. "Solvents."* Weinheim: Wiley-VCH Verlag GmbH & Co. KGaA, 2005.
24. de Jong V, Louw R. Performance of supported nickel and other metal catalysts in the hydrodechlorination of chlorobenzene and 1-chlorohexane. *Appl Catal A*. 2004;271:153–163.
25. Ukisu Y, Miyadera T. Hydrogen-transfer hydrodechlorination of polychlorinated dibenzo-p-dioxins and dibenzofurans catalyzed by supported palladium catalysts. *Appl Catal B*. 2003;40:141–149.
26. Yakovlev VA, Terskikh VV, Simagina VI, Likholobov VA. Liquid phase catalytic hydrodechlorination of chlorobenzene over supported nickel and palladium catalysts: an NMR insight into solvent function. *J Mol Catal Chem*. 2000;153:231–236.
27. Kopinke FD, Mackenzie K, Koehler R, Georgi A. Alternative sources of hydrogen for hydrodechlorination of chlorinated organic compounds in water on Pd catalysts. *Appl Catal A*. 2004;271:119–128.
28. Ukisu Y. Highly enhanced hydrogen-transfer hydrodechlorination and hydrogenation reactions in alkaline 2-propanol/methanol over supported palladium catalysts. *Appl Catal A*. 2008;349:229–232.
29. Marshall WD, Kubátová A, Lagadec AJM, Miller DJ, Hawthorne SB. Zero-valent metal accelerators for the dechlorination of pentachlorophenol (PCP) in subcritical water. *Green Chem*. 2002;4: 17–23.
30. Lide DR. *Handbook of Chemistry and Physics*, 87th ed. Boca Raton: Taylor and Francis, 2009.
31. Xia C, Xu J, Wu W, Luo Q, Chen J, Zhang Q, Liang X. Catalytic hydrodechlorination of 2,4,4′-trichloro-2′-hydroxyphenylether under mild conditions. *Appl Catal B*. 2003;45:281–292.
32. Mackenzie K, Frenzel H, Kopinke FD. Hydrodehalogenation of halogenated hydrocarbons in water with Pd catalysts: reaction rates and surface competition. *Appl Catal B*. 2006;63:161–167.
33. Yuan G, Keane MA. Aqueous-phase hydrodechlorination of 2,4-dichlorophenol over Pd/Al_2O_3: reaction under controlled pH. *Ind Eng Chem Res*. 2007;46:705–715.
34. Dollimore D, Heal GR. Pore-size distribution in typical adsorbent systems. *J Colloid Interface Sci*. 1970;33:508–519.
35. Amorim C, Keane MA. Palladium supported on structured and non-structured carbon: a consideration of Pd particle size and the nature of reactive hydrogen. *J Colloid Interface Sci*. 2008;322:196–208.
36. Yuan G, Keane MA. Liquid phase catalytic hydrodechlorination of 2,4-dichlorophenol over carbon supported palladium: an evaluation of transport limitations. *Chem Eng Sci*. 2003;58:257–267.

37. Gómez-Quero S, Cárdenas-Lizana F, Keane MA. Effect of metal dispersion on the liquid phase hydrodechlorination of 2,4-dichlorophenol over Pd/Al_2O_3. *Ind Eng Chem Res*. 2008;47:6841–6853.
38. Shindler Y, Matatov-Meytal Y, Sheintuch M. Wet hydrodechlorination of p-chlorophenol using Pd supported on an activated carbon cloth. *Ind Eng Chem Res*. 2001;40:3301–3308.
39. Storsæter S, Tøtdal B, Walmsley JC, Tanem BS, Holmen A. Characterization of alumina-, silica-, and titania-supported cobalt Fischer-Tropsch catalysts. *J Catal*. 2005;236:139–152.
40. Sanchez-Valente J, Bokhimi X, Toledo JA. Synthesis and catalytic properties of nanostructured aluminas obtained by sol-gel method. *Appl Catal A*. 2004;264:175–181.
41. Trueba M, Trasatti SP. γ-Alumina as a support for catalysts: a review of fundamental aspects. *Eur J Inorg Chem*. 2005;17,3393–3403.
42. Shena L, Chen Z. Critical review of the impact of tortuosity on diffusion. *Chem Eng Sci*. 2007;62:3748–3755.
43. Jáuregui-Haza UJ, Pardillo-Fontdevila EJ, Wilhelm AM, Delmas H. Solubility of hydrogen and carbon monoxide in water and some organic solvents. *Lat Am Appl Res*. 2004;34:71–74.
44. Yen LC, McKetta JJ. A thermodynamic correlation of nonpolar gas solubilities in polar, nonassociated liquids. *AIChE J*. 1962;8:501–507.
45. Prausnitz JM, Shair FH. A thermodynamic correlation of gas solubilities. *AIChE J*. 1961;7:682–687.
46. Lemcoff NO. Liquid phase catalytic hydrogenation of acetone. *J Catal*. 1977;46:356–364.
47. Watson KM. Thermodynamics of the liquid state: generalized prediction of properties. *Ind Eng Chem*. 1943;35:398–406.
48. Mukherjee S, Vannice MA. Solvent effects in liquid-phase reactions I activity and selectivity during citral hydrogenation on Pt/SiO_2 and evaluation of mass transfer effects. *J Catal*. 2006;243:108–130.
49. Danner RP, Daubert TE. *Manual for Predicting Chemical Process Design Data*. New York: Design Institute for Physical Property Data, 1983.
50. King CJ, Hsueh L, Mao KW. Liquid phase diffusion of nonelectrolytes at high dilution. *J Chem Eng Data*. 1965;10:348–350.
51. Smith JM. *Chemical Engineering Kinetics*. Singapore: McGraw-Hill, 1981.
52. Keane MA. Hydrodehalogenation of haloarenes over silica supported Pd and Ni: a consideration of catalytic activity/selectivity and haloarene reactivity. *Appl Catal A*. 2004;271:109–118.
53. Alonso F, Beletskaya IP, Yus M. Metal-mediated reductive hydrodehalogenation of organic halides. *Chem Rev*. 2002;102:4009–4091.
54. Sengwa RJ, Abhilasha M. A comparative study of non-polar solvents effect on dielectric relaxation and dipole moment of binary mixtures of mono alkyl ethers of ethylene glycol and of diethylene glycol with ethyl alcohol. *J Mol Liq*. 2006;123:92–104.
55. Jouyban A, Soltanpour S, Chan HK. A simple relationship between dielectric constant of mixed solvents with solvent composition and temperature. *Int J Pharm*. 2004;269:353–360.
56. Sato T, Chiba A, Nozaki R. Dynamical aspects of mixing schemes in ethanol-water mixtures in terms of the excess partial molar activation free energy, enthalpy, and entropy of the dielectric relaxation process. *J Chem Phys*. 1999;110:2508–2521.
57. Goffredi F, Goffredi M, Liveri VT. Effect of tetrahydrofuran on the conductance and ion-pairing of hydrogen chloride in wet and dry methanol mixtures. *J Solution Chem*. 1995;24:813–826.
58. Sudo S, Shinyashiki N, Kitsuki Y, Yagihara S. Dielectric relaxation time and relaxation time distribution of alcohol-water mixtures. *J Phys Chem A*. 2002;106:458–464.
59. Sato T, Chiba A, Nozaki R. Composition-dependent dyna mical structures of monohydric alcohol-water mixtures studied by microwave dielectric analysis. *J Mol Liq*. 2002;96/97: 327–339.
60. Smith RL, Lee SB, Komori H, Arai K. Relative permittivity and dielectric relaxation in aqueous alcohol solutions. *Fluid Phase Equilib*. 1998;144:315–322.
61. Herráez JV, Belda R. Refractive indices, densities and excess molar volumes of monoalcohols + water. *J Solution Chem*. 2006; 35:1315–1328.
62. Nayak JN, Aralaguppi MI, Naidu BVK, Aminabhavi TM. Thermodynamic properties of water + tetrahydrofuran and water + 1,4-dioxane mixtures at 303.15, 313.15 and 323.15 K. *J Chem Eng Data*. 2004;49:468–474.
63. Chaudhari A, Khirade P, Singh R, Helambe SN, Narain NK, Mehrotra SC. Temperature dependent dielectric relaxation study of tetrahydrofuran in methanol and ethanol at microwave frequency using time domain technique. *J Mol Liq*. 1999;82:245–253.
64. Sengwa RJ, Madhvi Sankhla S, Sharma S. Characterization of heterogeneous interaction behaviour in ternary mixtures by a dielectric analysis: equi-molar H-bonded binary polar mixtures in aqueous solutions. *J Solution Chem*. 2006;35:1037–1055.
65. Marczak W, Spurek M. Compressibility and volume effects of mixing of 1-propanol with heavy water. *J Solution Chem*. 2004;33:99–116.
66. Pawar VP, Mehrotra SC. Dielectric relaxation study of chlorobenzene with formamide at microwave frequency using time domain reflectometry. *J Mol Liq*. 2004;115:17–22.

Manuscript received Apr. 7, 2009, and revision received Jun. 23, 2009.